THE JOURNAL OF BIOLOGICAL CHEMISTRY VOL. 285, NO. 51, pp. 39710–39717, December 17, 2010

Functional Properties of the *Arabidopsis* Peptide Transporters AtPTR1 and AtPTR5*[S]

Received for publication, May 18, 2010, and in revised form, September 28, 2010 Published, JBC Papers in Press, October 11, 2010, DOI 10.1074/jbc.M110.141457

Ulrich Z. Hammes[‡1,2], Stefan Meier[‡1], Daniela Dietrich[‡3], John M. Ward[§], and Doris Rentsch[‡4]

From the [‡]Institute of Plant Sciences, University of Bern, Altenbergrain 21, 3013 Bern, Switzerland and the [§]Department of Plant Biology, University of Minnesota, St. Paul, Minnesota 55108

The *Arabidopsis* di- and tripeptide transporters AtPTR1 and AtPTR5 were expressed in *Xenopus laevis* oocytes, and their selectivity and kinetic properties were determined by voltage clamping and by radioactive uptake. Dipeptide transport by AtPTR1 and AtPTR5 was found to be electrogenic and dependent on protons but not sodium. In the absence of dipeptides, both transporters showed proton-dependent leak currents that were inhibited by Phe-Ala (AtPTR5) and Phe-Ala, Trp-Ala, and Phe-Phe (AtPTR1). Phe-Ala was shown to reduce leak currents by binding to the substrate-binding site with a high apparent affinity. Inhibition of leak currents was only observed when the aromatic amino acids were present at the N-terminal position. AtPTR1 and AtPTR5 transport activity was voltage-dependent, and currents increased supralinearly with more negative membrane potentials and did not saturate. The voltage dependence of the apparent affinities differed between Ala-Ala, Ala-Lys, and Ala-Asp and was not conserved between the two transporters. The apparent affinity of AtPTR1 for these dipeptides was pH-dependent and decreased with decreasing proton concentration. In contrast to most proton-coupled transporters characterized so far, $-I_{max}$ increased at high pH, indicating that regulation of the transporter by pH overrides the importance of protons as co-substrate.

Transporters for di- and tripeptides are found in bacteria, fungi, plants, and animals (1–4). The majority of the bacterial peptide transporters characterized so far belong to the ATP-binding cassette transporter family (5). Some prokaryotic as well as most of the di- and tripeptide transporters of eukaryotes are members of the PTR[5]/NRT1 (peptide transporter/nitrate transporter 1) family (1, 3), which belongs to the major facilitator superfamily (6). In plants, the PTR/NRT1 gene family is much larger than in other kingdoms and consists of 53 genes in *Arabidopsis* (3). Functional di-/tripeptide transport has been shown for members from *Arabidopsis* (AtPTR1, AtPTR2, AtPTR3, and AtPTR5 (2, 3, 7)), faba bean (VfPTR1 (8)), barley (HvPTR1 (9)), and *Hakea actites* (HaPTR4 (10)). For most plant PTR/NRT1 proteins, the substrate selectivity has not been determined yet, but it is clear that some transport substrates other than peptides. For example, various *Arabidopsis* PTR/NRT1 members mediate low affinity uptake or export of nitrate (3, 11). Furthermore, a nitrate/histidine transporter from *Brassica napus* (BnNRT1;2 (12)) and a carboxylate transporter from alder were functionally characterized (13), and a chloroplast nitrite transporter was described (14).

In other kingdoms, only a few members of the PTR/NRT1 family are present, which primarily mediate proton-coupled transport of di- and tripeptides, as well as structurally related compounds (15). In mammals, four peptide transporters (PepT1, PepT2, PHT1, and PHT2) show 21–28% amino acid identity to AtPTR1, AtPTR2, and AtPTR5, whereas sequence identity among these three plant transporters is 59–74% (supplemental Table 1). Two of the four mammalian peptide transporters mediate transport of free histidine, in addition to di- and tripeptides (16). The transporters from rat and human have been investigated in detail; one of the mammalian transporters mediates uptake of peptides in the small intestine functioning as a main pathway for the absorption of dietary nitrogen (17). Moreover, mammalian PEPT1 and PEPT2 also transport modified peptides, including β-lactam antibiotics, enzyme inhibitors, and other peptide-like drugs (15).

Studies on the substrate selectivity of PEPT1 and PEPT2, using peptides with proteinogenic amino acids and natural peptides, as well as pharmacologically interesting compounds with a similar structure (>350 different compounds (15)), confirmed the predicted low selectivity. That work also revealed important features of compounds to be recognized as substrates by PEPT1 and/or PEPT2 (15, 16). The substrate selectivity of plant peptide transporters has been investigated only for *Arabidopsis* AtPTR1 and AtPTR2, which, like the mammalian transporters, recognize a large number of di- and tripeptides with moderate to high apparent affinity (18–20). Affinity of AtPTR2 is dependent on both the N- and C-terminal amino acids and is largely independent of the membrane potential (18). Chiang *et al.* (18) also established that AtPTR2 transports peptides and protons simultaneously by a random binding mechanism.

* This work was supported by Swiss National Science Foundation Grants 31003A_127340 and 3100A0-107507 (to D. R.) and United States Department of Energy Grant DE-FG02-07ER15886 (to J. M. W.).

[S] The on-line version of this article (available at http://www.jbc.org) contains supplemental Table 1 and Figs. 1–3.

[1] Both authors contributed equally to this work.

[2] Present address: Dept. of Cell Biology and Plant Biochemistry, University of Regensburg, Universitätsstrasse 31, 93053 Regensburg, Germany.

[3] Present address: Division of Plant and Crop Science, University of Nottingham, Sutton Bonington Campus, Loughborough, LE12 5RD, United Kingdom.

[4] To whom correspondence should be addressed: Institute of Plant Sciences, University of Bern, Altenbergrain 21, 3013 Bern, Switzerland. Fax: 41-31-631-4942; E-mail: doris.rentsch@ips.unibe.ch.

[5] The abbreviations used are: PTR, peptide transporter; TEVC, two-electrode voltage clamping; CHES, 2-(cyclohexylamino)ethanesulfonic acid.

Transporters for di/tripeptides have important functions in plants. Experiments using antisense repression of *AtPTR2* showed the importance of peptide transport for flowering and seed development (21). Furthermore, work with knock-out mutants (*atptr1* and *atptr5*) and overexpression lines (35S-*AtPTR5*) demonstrated that AtPTR5 facilitates peptide transport into germinating pollen and possibly into maturating pollen, ovules, and seeds and provided evidence that peptide transporters facilitate uptake of nitrogen from the rhizosphere (7). These physiological functions indicated a role in transport of protein degradation products, which is consistent with the low selectivity of these transporters for different di- and tripeptides.

Detailed knowledge of transport characteristics and kinetics is essential to understand the physiological role *in planta*. Here, we report the comprehensive characterization of the biochemical properties of AtPTR1 and AtPTR5 using heterologous expression in *Xenopus* oocytes and two-electrode voltage clamping (TEVC). The results show functional similarities and differences between these two peptide transporters as well as profound differences compared with the properties of AtPTR2.

EXPERIMENTAL PROCEDURES

cRNA Synthesis—The *AtPTR5* cDNA was isolated from pUC18-GFP5Tsp (7) using BglII and SalI, blunt-ended using Klenow, and inserted into the SmaI site of pBF1 (22). The resulting construct as well as pOO2-*AtPTR1* (19) was linearized using MluI. cRNA was synthesized using the Ambion Sp6 mMessage mMachine kit (Ambion, Austin, TX).

Preparation of Oocytes—Stage V or VI oocytes from *Xenopus laevis* females were surgically removed, manually separated into clusters of around 10 oocytes, and defolliculated by incubation in 5 ml of Barth's solution containing 11–50 mg of collagenase for 1.5 to 3 h at room temperature. When >70% of the oocytes were separated, collagenase solution was removed, and the oocytes were washed six times with 1 mg ml^{-1} BSA in Barth's solution (88 mM NaCl, 1 mM KCl, 0.33 mM $Ca(NO_3)_2$, 0.41 mM $CaCl_2$, 82 mM $MgCl_2$, 2.4 mM $NaHCO_3$, 10 mM HEPES, pH 7.6, with NaOH).

RNA Injection—Oocytes were injected with 50 nl of cRNA (50 ng) and stored in Barth's solution containing 50 μg ml^{-1} gentamycin, 100 μg ml^{-1} streptomycin, and 100 units ml^{-1} penicillin at 15 °C. Recordings were done 4–6 days after injection. Pipettes for injection and recording were pulled using a model P-30 or P-87 puller (Sutter Instrument Co., Novato, CA).

Setup—1.5-mm (outer diameter) thin wall borosilicate glass (Warner Instrument Corp., Hamden, CT) was used for recordings. Pipettes were filled with 1 M KCl and connected to the head stage with a chlorided silver wire. Pipette resistance was 1.5–3.5 megohms in modified Ringer's solution (115 mM NaCl, 2 mM KCl, 1.8 mM $CaCl_2$, 1 mM $MgCl_2$, 5 mM MES for pH 5.5 to pH 6.5, 5 mM HEPES for pH 7 to pH 8.5, 5 mM CHES for pH 9 to pH 10).

Experiments to determine co-transport of Na^+ were performed in buffer containing 1.8 mM $CaCl_2$, 1 mM $MgCl_2$, 5 mM MES (for pH 5.5) or 5 mM HEPES (for pH 7.5) and NaCl and choline chloride in the following concentrations: 0 mM NaCl buffer (0 mM NaCl, 117 mM choline chloride), 50 mM NaCl buffer (50 mM NaCl, 67 mM choline chloride), 100 mM NaCl buffer (100 mM NaCl, 17 mM choline chloride). Substrates were added to the buffer solutions as indicated, and the necessary pH adjustments were made. All peptide substrates were purchased from Bachem (Burgdorf, Switzerland).

TEVC was done using a Dagan TEVC-200A amplifier (Dagan Corp., Minneapolis, MN) or a Warner oocyte clamp OC-725C (Warner Instrument Corp., Hamden, CT). Currents were recorded via an LM12 interface (Dagan Corp.) using Clampex (Axon Instruments Inc., Union City, CA).

Two protocols were used to measure steady-state inward currents. (i) The oocyte membrane potential was clamped at −40 mV, and currents induced in response to the addition of peptides were continuously monitored by using a chart recorder or MiniDigi 1A/Axoscope 9.2 (Axon Instrument Corp., Union City, CA). (ii) The oocyte plasma membrane was held at −40 mV, and membrane currents were measured after stepping from the holding potential (V_h) to test potentials (V_m) between −140 and +20 mV in 20-mV increments. Each voltage pulse was applied for 250 ms. Currents were filtered at 5000 Hz. Steady-state peptide-induced currents were obtained by calculating the amplitude of steady-state currents between 160 and 200 ms using Clampfit. Steady-state currents in the absence of substrate were measured before and after supplying the peptide. The two datasets were averaged and subtracted from the data obtained in the presence of substrate. Currents were normalized to currents for 500 μM Ala-Ala (at pH 5.5) determined before each experiment to account for different expression levels between oocytes.

The effects of substrate concentration on the steady-state kinetics were determined by nonlinear curve fitting of the induced currents (I) to the Michaelis-Menten Equation 1,

$$I = \frac{I^S_{max} \cdot [S]}{K^S_{0.5} + [S]} \quad \text{(Eq. 1)}$$

where S is the substrate; I^S_{max} is the maximal substrate-induced current and $K^S_{0.5}$ is the substrate concentration at half I^S_{max} (half-maximal concentration). Curve fittings were performed using SigmaPlot (SPSS Science, Chicago). Values represent mean ± S.E. of at least three oocytes from at least two batches of oocytes.

Ala-Ala Uptake Assay—After injection, oocytes were stored for 5 days at 15 °C. Six oocytes were preincubated for 5 min in modified Ringer's solution (115 mM NaCl, 2 mM KCl, 1.8 mM $CaCl_2$, 1 mM $MgCl_2$, and 5 mM MES for pH 5.5 or 5 mM HEPES for pH 7.5) and then transferred to 500 μl of modified Ringer's solution (pH 5.5 or pH 7.5) with 254 μM L-[^{3}H]Ala-Ala (291 Bq $nmol^{-1}$) and incubated for 1 h at room temperature. Subsequently, oocytes were washed two times in ice-cold modified Ringer, pH 7.5, containing 1 mM unlabeled Ala-Ala and five times in ice-cold modified Ringer, pH 7.5, without Ala-Ala. Oocytes were lysed in 2% SDS for 25 min at room temperature, before scintillation mixture (ULTIMA GOLD™ XR, PerkinElmer Life Sciences) was added, and the samples

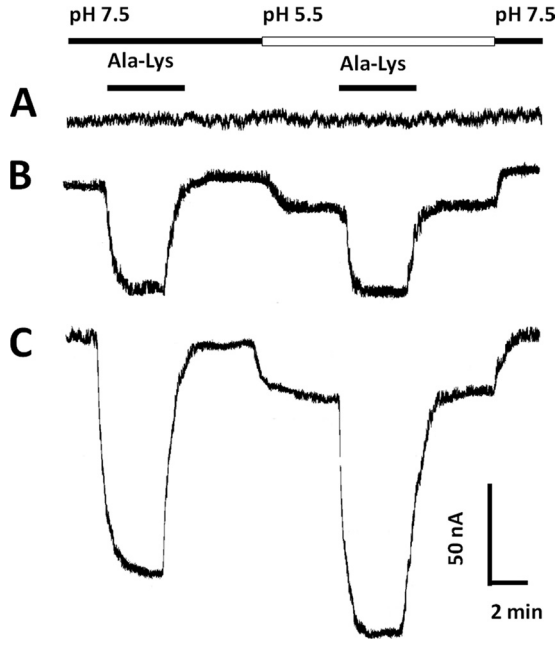

FIGURE 1. **Dipeptide-evoked currents in oocytes expressing AtPTR1 and AtPTR5.** Oocytes were superfused with modified Ringer's solution, pH 7.5 or pH 5.5, and clamped at a membrane potential of −60 mV. 1 mM Ala-Lys was added and removed at the times indicated by the *bar above* the trace. Results from single oocytes are shown for water-injected (*A*), AtPTR5- (*B*), and AtPTR1 (*C*)-expressing oocytes.

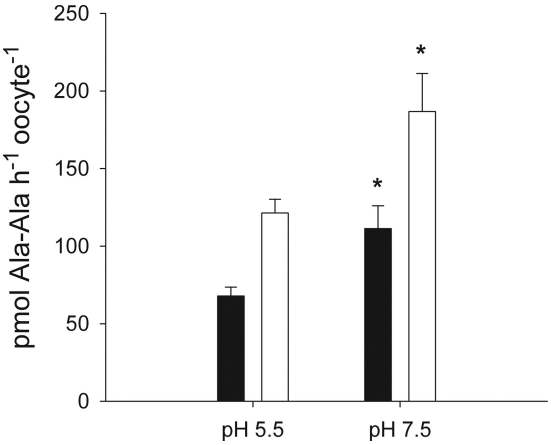

FIGURE 2. **Uptake of [^{3}H]Ala-Ala in AtPTR1- and AtPTR5-expressing oocytes at high and low pH.** Uptake of [^{3}H]Ala-Ala was determined in AtPTR1- (*black*) and AtPTR5 (*white*)-injected oocytes for 1 h at pH 5.5 and pH 7.5 (± S.E.; $n = 6$). Student's *t* test was performed, and *asterisks* indicate significant differences, $p < 0.05$, between transport rates at pH 5.5 and pH 7.5.

TABLE 1

Apparent affinities of AtPTR1 and AtPTR5 for different dipeptides at pH 5.5, measured at V_m −140 mV and V_m −60 mV

Values represent mean ± S.E. of at least three oocytes.

	$K_{0.5}$ (μM) at $V_m = -140$ mV			$K_{0.5}$ (μM) at $V_m = -60$ mV		
	Ala-Ala	Ala-Lys	Ala-Asp	Ala-Ala	Ala-Lys	Ala-Asp
AtPTR1	57 ± 2	142 ± 12	409 ± 17	58 ± 3	247 ± 38	632 ± 112
AtPTR5	23 ± 4	167 ± 12	129 ± 4	19 ± 3	134 ± 9	71 ± 6

were counted. Ala-Ala uptake of water-injected oocytes (50–60 pmol of Ala-Ala h^{-1} $oocyte^{-1}$ at pH 5.5 and 7.5) was subtracted from uptake rates of AtPTR1- or AtPTR5-expressing oocytes.

Yeast Growth, Transformation, and Selection—Transformation, growth, and transport assays using *Saccharomyces cerevisiae* strain LR2 (*MATα hip1-614 his4-401 can1 ino1 ura3-52 ptr2*Δ::*hisG* (20)) were performed as described earlier (20).

RESULTS

Dipeptide-induced currents were analyzed in *X. laevis* oocytes injected with *AtPTR1* or *AtPTR5* cRNA using TEVC. At pH 7.5 and pH 5.5, the addition of 1 mM Ala-Lys to AtPTR5- or AtPTR1-expressing oocytes induced inward currents (Fig. 1, *B* and *C*). Current amplitude was dependent on the batch of oocytes and time after RNA injection. No dipeptide-induced currents were detected in water-injected oocytes (Fig. 1*A*). The addition of 1 mM Ala-Ala also induced inward currents (data not shown). As Ala-Ala is present in its zwitterionic form at pH 5.5, the induced inward current indicates a co-transport of cations. Ala-Ala transport was confirmed using radio-tracer flux experiments in AtPTR1- and AtPTR5-expressing oocytes, which accumulated [^{3}H]Ala-Ala (Fig. 2). Furthermore, under TEVC inward (leak) currents were observed when the pH was shifted from pH 7.5 to pH 5.5 in AtPTR5- and AtPTR1-injected oocytes in the absence of substrate (Fig. 1, *B* and *C*). These results are consistent with a co-transport of protons and peptides as described for AtPTR2 and the mammalian peptide transporters (16, 18).

Dependence of Apparent Affinity and Maximal Transport Rate on Membrane Potential—The dependence of $K_{0.5}$ and I_{max} on the membrane potential was determined in the range of V_m −140 to +20 mV for both AtPTR1 and AtPTR5. Ala-Ala, Ala-Lys, and Ala-Asp were chosen as representatives for neutral, cationic, and anionic dipeptides. At a membrane potential of −140 mV and pH 5.5, the apparent affinity of AtPTR5 was determined as $K_{0.5}^{Ala\text{-}Ala}$ 23 ± 4 μM, $K_{0.5}^{Ala\text{-}Lys}$ 167 ± 12 μM, and $K_{0.5}^{Ala\text{-}Asp}$ 129 ± 4 μM, respectively (Table 1), the latter two affinities were thus comparable with the apparent affinity of AtPTR5 for Ala-Lys ($K_{0.5}^{Ala\text{-}Lys}$ 163 μM) and Ala-Asp ($K_{0.5}^{Ala\text{-}Asp}$ 131 μM) determined previously ($n = 4$ oocytes (7)) and similar to the apparent affinity of AtPTR1 for these dipeptides determined under comparable experimental conditions (19). At pH 5.5, $K_{0.5}$ of AtPTR1 for Ala-Lys decreased with more negative membrane potentials, whereas the apparent affinity for Ala-Ala was not affected by the membrane potential, and $K_{0.5}^{Ala\text{-}Asp}$ was lower at less negative membrane potentials (Fig. 3*A*). In contrast, $K_{0.5}$ of AtPTR5 was constant for Ala-Ala and Ala-Lys and increased with more negative membrane potential for Ala-Asp (Fig. 3*C*). On the other hand $-I_{max}$ increased at more negative membrane potentials for all three dipeptides in both AtPTR- and AtPTR5-injected oocytes (Fig. 3, *B* and *D*).

Apparent Affinity and Maximal Transport Rates Are Dependent on the Proton Concentration—Apparent affinity and I_{max} were dependent on the proton concentration. Measurements for AtPTR1 revealed that at a membrane potential of −140 mV $K_{0.5}$ decreased with increasing proton concentration for all three dipeptides (Fig. 4, *A–C*). Similarly, $-I_{max}$ for

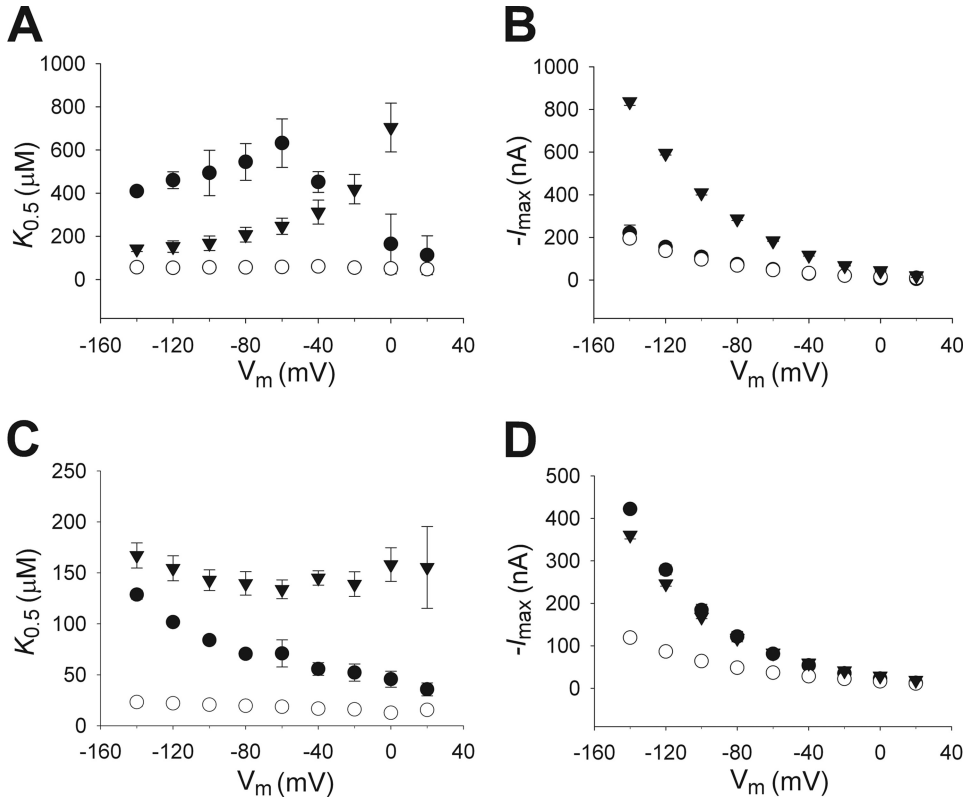

FIGURE 3. **Voltage dependence of $K_{0.5}$ and $-I_{max}$ in AtPTR1- and AtPTR5-injected oocytes at pH 5. 5.** Voltage dependence of $K_{0.5}$ (*A* and *C*) and $-I_{max}$ (*B* and *D*) was determined at 3.2 μM $[H^+]_{out}$ for AtPTR1- (*A* and *B*) and AtPTR5 (*C* and *D*)-injected oocytes. For each oocyte, currents were normalized to the current induced by 500 μM Ala-Ala at pH 5.5 and a membrane potential of −140 mV. Values represent mean ± S.E. of at least three oocytes. ○, Ala-Ala; ▼, Ala-Lys; ●, Ala-Asp.

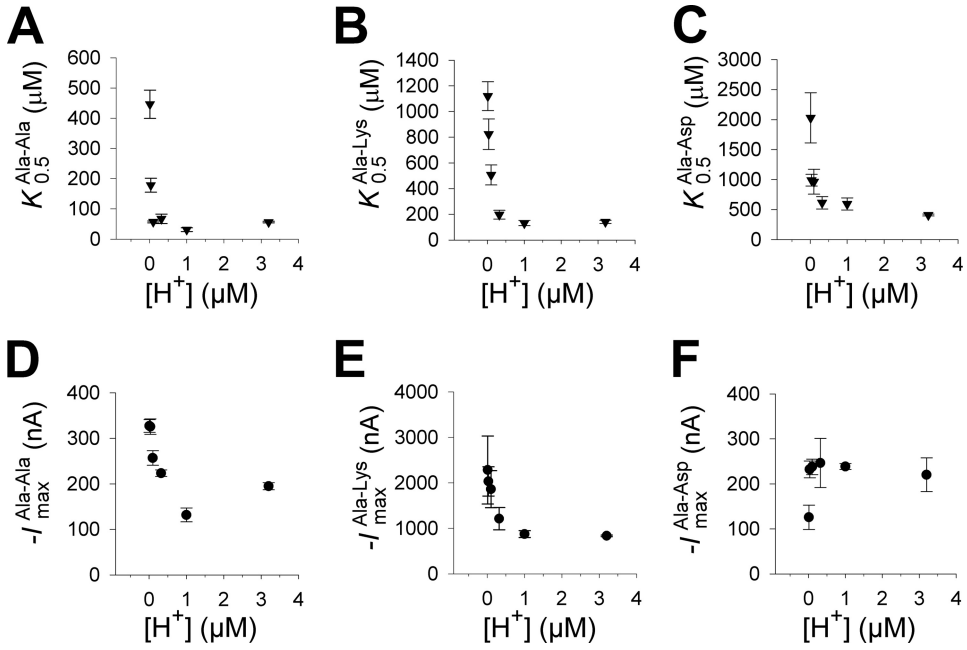

FIGURE 4. **Dependence of $K_{0.5}$ and $-I_{max}$ of AtPTR1 on pH.** $K_{0.5}$ (*A–C*) and $-I_{max}$ (*D–F*) values of AtPTR1 for Ala-Ala (*A* and *D*), Ala-Lys (*B* and *E*), and Ala-Asp (*C* and *F*) were determined at V_m of −140 mV and increasing proton concentrations. Values are mean ± S.E. from at least three oocytes.

Ala-Ala and Ala-Lys decreased with increasing proton concentration (Fig. 4, *D* and *E*). Only $-I_{max}$ of Ala-Asp was not changed by pH over a broad range and sharply decreased at very low proton concentrations, indicating that the aspartate residue in Ala-Asp might be transported in its protonated form (Fig. 4*F*). AtPTR5 also showed higher currents at saturating concentrations of Ala-Ala at high pH (pH 7.5) (Fig. 5), demonstrating that higher transport rates at low proton concentrations is a common feature of both transporters and possibly other transporters of this clade. This trend was robust

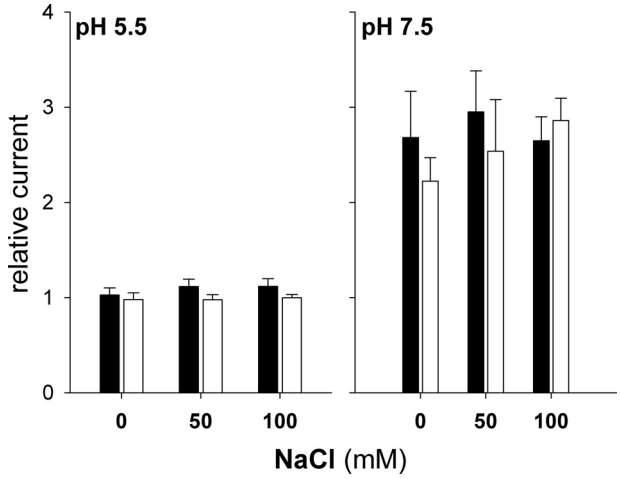

FIGURE 5. **Dependence of Ala-Ala transport on pH and sodium chloride.** Ala-Ala (1 mM)-induced currents were determined at pH 7.5 and 5.5 in the presence of increasing concentrations (0, 50, and 100 mM) of NaCl in AtPTR1- (*black bars*) and AtPTR5 (*white bars*)-injected oocytes (±S.E.; $n = 3$; V_m −140 mV). Substrate-induced currents were normalized to 500 μM Ala-Ala-induced currents at pH 5.5 in sodium-free Ringer's solution and V_m −140 mV set at 1.

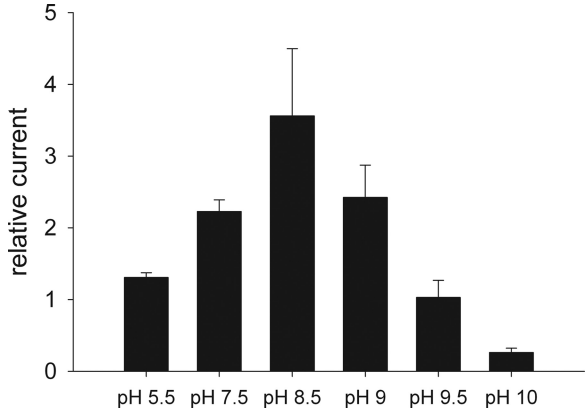

FIGURE 6. **AtPTR1-mediated Ala-Ala transport at high pH.** The currents induced by 10 mM Ala-Ala were determined at pH 5.5 and between pH 7.5 and pH 10 in oocytes expressing AtPTR1 (V_m −140 mV). Substrate-induced currents were normalized on 500 μM Ala-Ala-induced currents at pH 5.5 set at 1.

until pH 8.5 was reached, whereas at higher pH values, 10 mM Ala-Ala-induced currents decreased considerably (Fig. 6). This suggests that within the physiological range, the intrinsic pH dependence of the transporter itself overrules the dependence on protons as co-substrate.

Voltage dependence of peptide transport was also influenced by the proton concentration. Maximum transport rates of AtPTR1-mediated dipeptide transport decreased supralinearly with hyperpolarizing voltages at pH 5.5 (Fig. 3*B*), 6.5, and 7.5 (supplemental Fig. 1). At all membrane potentials, I_{max} was most negative at high pH for Ala-Ala and Ala-Lys and similar at all pH values for Ala-Asp. Although at pH 5.5 a decrease in apparent affinity at depolarized voltages was only shown for Ala-Lys (Fig. 3*A*), at pH 7.5 this effect was observed for all three dipeptides (supplemental Fig. 1).

To test whether higher $-I_{max}$ values at high pH were mediated by co-transport of Na^+ instead of H^+, currents induced by 1 mM Ala-Ala were measured at pH 5.5 and 7.5 in the presence of different concentrations of NaCl (Fig. 5). Increasing the Na^+ concentration did not change currents of AtPTR1-injected oocytes at both high and low pH and slightly increased Ala-Al- induced currents for AtPTR5 at pH 7.5, indicating that elevated substrate-induced current at high pH was due to pH regulation of the transporter rather than Na^+ replacing H^+ as the coupling ion. This was confirmed by experiments showing that at pH 7.5, both AtPTR1- and AtPTR5-expressing oocytes accumulated significantly more [^{3}H]Ala-Ala than at low pH (pH 5.5) (Fig. 2).

TABLE 2
Effects of inhibitors on AtPTR1- and AtPTR5-mediated Ala-Ala uptake rates in *S. cerevisiae*

Uptake rates of 20 μM Ala-Ala were determined at pH 4.5 in the presence of different inhibitors. Uptake in the absence of inhibitors was taken as 100% and corresponds to 20.9 ± 0.6 (AtPTR1) and 17.4 ± 0.2 (AtPTR5) pmol of Ala-Ala min^{-1} 10^{-6} cells. Data represent means ± S.E. (n = 3). Inhibitors were added 6 min before the transport assay. CCCP is carbonyl cyanide *m*-chlorophenylhydrazone; NEM is *N*-ethylmaleimide; DEPC is diethyl pyrocarbonate.

Inhibitor	AtPTR1 relative uptake	AtPTR5 relative uptake
	%	%
None	100	100
10 mM CCCP	26.16 ± 2.3	20.48 ± 1.7
1 mM NEM	12.46 ± 1.0	14.00 ± 2.0
1 mM DEPC	0.42 ± 0.2	0.55 ± 0.2

To further examine the nature of the coupling ion and the functional groups involved in substrate binding or transport, AtPTR1 and AtPTR5 were expressed in *S. cerevisiae* and Ala-Ala transport rates determined in the presence of various well established inhibitors (Table 2). Carbonyl cyanide *m*-chlorophenylhydrazone, a protonophore, reduced uptake rates of [^{3}H]Ala-Ala by AtPTR1 and AtPTR5 to 26 and 20%, respectively, consistent with protons as coupling ions. [^{3}H]Ala-Ala uptake by both transporters was sensitive to the sulfhydryl group-modifying agent *N*-ethylmaleimide, similar to the effect of this inhibitor on AtPTR2 (20), and also diethyl pyrocarbonate, a histidyl-modifying agent, reduced uptake rates of [^{3}H]Ala-Ala of both transporters to ~1%.

AtPTR1 and AtPTR5 Have Different Substrate Selectivity—Previous analyses of substrate selectivity showed that AtPTR1 recognized di- and tripeptides with different composition of the side chains (19). Here, we analyzed the ability of AtPTR1 and AtPTR5 to recognize dipeptides with different hydrophobic or aromatic amino acids at the N- or C-terminal position. At a concentration of 1 mM dipeptide, V_m −140 mV, and pH 5.5, the currents induced by various substrates differed considerably (Fig. 7). Whereas Ala-Ile and Ile-Ala induced comparable currents in AtPTR5-injected oocytes, Ile-Ala was transported more efficiently than Ala-Ile by AtPTR1. Ala-containing dipeptides with the aromatic amino acids Trp or Phe induced inward currents only when the hydrophobic residue was at the C-terminal position. Tyr-Ala also induced less current than Ala-Tyr in both AtPTR1- and AtPTR5-injected oocytes. The exception was Phe-Phe, which induced currents comparable with Ala-Ala or Ala-Phe in AtPTR5 but not in AtPTR1-expressing oocytes. Transport of Ala-Phe, Phe-Ala, and Phe-Phe was dependent on pH and was considerably higher at low proton concentrations (Fig. 8).

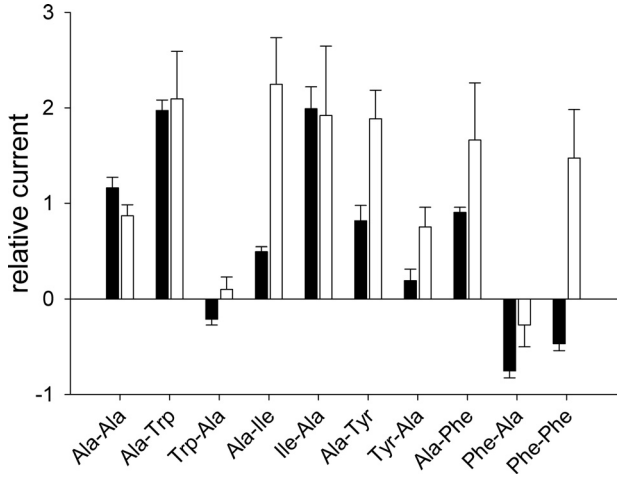

FIGURE 7. **Substrate selectivity of AtPTR1 and AtPTR5 for dipeptides with hydrophobic or aromatic residues.** 1 mM dipeptide-induced currents were determined at V_m −140 mV and pH 5.5 in AtPTR1- (*black bars*) and AtPTR5 (*white bars*)-injected oocytes. No current was detected when these substrates were tested in control oocytes (data not shown). Currents were normalized on 500 μM Ala-Ala-induced current at pH 5.5 set at 1. Values are mean ± S.E. (AtPTR1, $n = 3–5$; AtPTR5, $n = 3–6$).

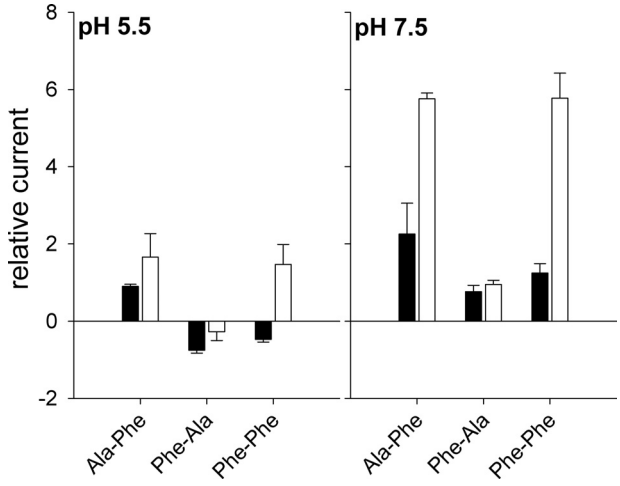

FIGURE 8. **pH dependence of Ala-Phe, Phe-Ala, and Phe-Phe transport.** 1 mM Ala-Phe-, Phe-Ala-, and Phe-Phe-induced current was determined at V_m −140 mV and pH 5.5 and 7.5 in AtPTR1- (*black bars*) and AtPTR5 (*white bars*)-injected oocytes. Values are mean ± S.E. ($n \geq 3$ oocytes). All currents were normalized to currents recorded with 500 μM Ala-Ala at pH 5.5, V_m −140 mV, for each oocyte. Data for pH 5.5 are extracted from Fig. 6.

Surprisingly, and in contrast to Ala-Phe, at pH 5.5 the dipeptide Phe-Ala but also Trp-Ala and Phe-Phe reduced the background leak current in AtPTR1-expressing oocytes (Fig. 7). Interestingly, the Phe-Ala- and Phe-Phe-induced reduction of the leak current was pH-dependent and could not be observed at pH 7.5 (Fig. 8). The Phe-Ala-mediated reduction in current was concentration-dependent and could be described by Michaelis-Menten kinetics. The apparent affinity of the Phe-Ala-induced reduction of the leak current was 9.2 ± 1.8 μM ($n = 3$ oocytes; Fig. 9*A*). To test if the reduction is due to occupation of the substrate-binding site, the inhibition constant, K_i (*i.e.* 50% reduction of Ala-Lys induced current at its $K_{0.5}$ [100 μM] (19)), was determined by increasing concentrations of Phe-Ala to be 24.2 ± 3.3 μM (Fig. 9*B*). These results indicate that Phe-Ala is indeed recognized by

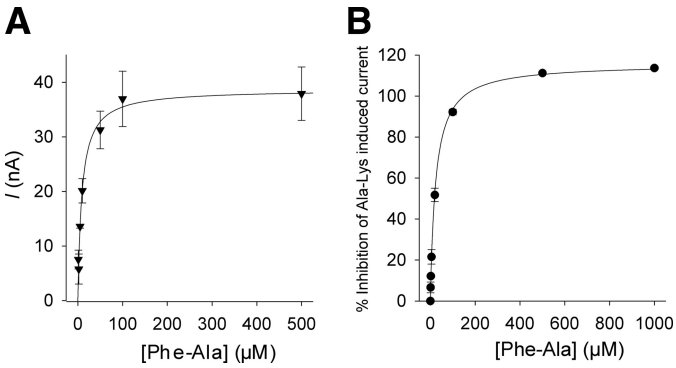

FIGURE 9. **Recognition of Phe-Ala by AtPTR1.** *A,* reduction of leak current in the absence of substrate at V_m −140 mV and pH 5.5 by increasing concentrations of Phe-Ala follows a Michaelis-Menten kinetic ($K_{0.5}$ 9.2 ± 1.8 μM). *B,* competition of Ala-Lys (100 μM)-induced current in the presence of increasing concentrations of Phe-Ala, K_i 24.2 ± 3.3 μM. Values are mean ± S.E. of at least three oocytes.

AtPTR1 with high apparent affinity, even though it does not seem to be transported at pH 5.5. In oocytes expressing AtPTR5, only Phe-Ala reduced the leak current, whereas Trp-Ala induced small inward currents, and Phe-Phe currents were comparable with Ala-Phe-induced currents. This indicates both differences but also common characteristics in substrate recognition of peptide transporters of this clade.

Results from *S. cerevisiae* strain LR2 expressing AtPTR1 or AtPTR5 showed that both Ala-Phe and Phe-Ala inhibited growth on His-Ala as a sole source of histidine (data not shown). This independently supports the finding that Phe-Ala interacts with the substrate-binding site and not only blocks leak currents.

DISCUSSION

Peptide transporters are generally considered to play a role in translocation of peptides generated by protein degradation. Because di- and tripeptides produced by protein hydrolysis vary in size, charge, and hydrophobicity, it is expected that these transporters have a low selectivity regarding the composition of the side chains. Chiang *et al.* (18) showed that the $K_{0.5}$ of AtPTR2 for most neutral peptides is in the range of 50–400 μM and is 1830 μM for Ala-Asp (pH 5.5 and V_m 60 mV). The affinities of AtPTR1 and AtPTR5 were in a similar range for Ala-Ala and Ala-Lys, although the apparent affinity for Ala-Asp was higher than shown for AtPTR2 (*i.e.* at pH 5.5, V_m −60 mV $K_{0.5}^{\text{Ala-Asp}}$: AtPTR5 71 μM, AtPTR1 632 μM; pH 5.5, V_m −140 $K_{0.5}^{\text{Ala-Asp}}$: AtPTR5 129 μM, AtPTR1 409 μM ((7, 18, 19), see Table 1 for comprehensive overview of the kinetic parameters at different membrane potentials).

For AtPTR1 and AtPTR5, higher dipeptide-induced currents were observed when the aromatic amino acids Trp, Tyr, or Phe were present at the C-terminal position. Ile-Ala was transported as efficiently as Ala-Ile in AtPTR5 but not in AtPTR1-injected oocytes, indicating slight differences in substrate recognition. Unexpectedly, some of the dipeptides with an aromatic amino acid at the N-terminal position did not induce inward currents but rather reduced the leak current observed at pH 5.5 in a concentration-dependent manner and thereby provided evidence that the leak current originated from the flow of the co-transported ion (Figs. 7 and 9).

Whether the block of the leak current is due to the inhibition of the conformational changes required to facilitate transport into the cell, to masking of the proton-binding site, or whether the (high affinity) binding of Phe-Ala prevents substrate translocation or hinders a coordinated release of both substrates remains elusive. A model illustrating the reduction of the leak current is presented in supplemental Fig. 2.

The Phe-Ala-induced reduction of the leak current could be competed for by Ala-Lys (Fig. 9), also in a concentration-dependent manner. This showed that binding of Ala-Lys, which is transported, and Phe-Ala, which is not, occurs at the same binding site. This finding was supported by results using a peptide transport-deficient and histidine auxotroph *S. cerevisiae* mutant expressing AtPTR1 or AtPTR5, which showed growth inhibition on medium containing Ala-His as sole source of histidine in the presence of Phe-Ala. It was somewhat surprising that AtPTRs can be blocked by a possible substrate. The concentration of peptides with an aromatic amino acid in the N-terminal position *in vivo* is unknown, but due to the lower abundance of amino acids with aromatic residues, it is probably quite low. Furthermore, because the excess of other peptide substrates could easily outcompete the inhibition, this inhibition might not be significant *in vivo*.

Studies on *Lactococcus lactis* DtpT (25) and on substrate affinities of peptide transporters in kidney (26) showed that increasing hydrophobicity in both the N- and C-terminal side chains increased the apparent affinity of a dipeptide substrate. Such a clear relation was not found for AtPTR2 (18). Nevertheless, these transporters all had the highest affinity for dipeptides with Phe and Leu residues. However, none of the dipeptides was reported to block transport of any of these transporters. Furthermore, leak current was only shown in mammalian PEPT2 (27), but it was not described for PEPT1 or AtPTR2 (18, 28). The leak current observed in PEPT2 was described to be due to the inward movement of coupling ions, *i.e.* protons (27). Our studies also suggest that AtPTR1 and AtPTR5 work as proton-coupled symporters, as sodium ions did not substitute for protons.

A noteworthy difference in transport activity between AtPTR1 and AtPTR5 concerned the dipeptide Phe-Phe. Although Phe-Phe was recognized by both transporters and was transported by AtPTR5, it was not transported by AtPTR1 and blocked the coupling ion leak similarly to Phe-Ala. The reason for this difference remains to be investigated. Only 26% of the amino acids (*i.e.* 147) differ between AtPTR1 and AtPTR5. Any differences observed with respect to transport properties and substrate selectivity, *e.g.* Phe-Phe recognition, can thus be attributed to these amino acids. Important residues might be identified in further studies using mutagenesis.

For AtPTR1 and AtPTR5, peptide-induced currents were strongly dependent on the membrane potential and increased supralinearly with more negative values for all substrates at all pH values tested. Membrane potentials in plants are usually between −100 and −150 mV, although potentials as low as −250 mV were also measured (29, 30). Consistently, the dipeptide-induced currents never saturated at the potentials applied (≤ −140 mV), which is a common feature among many transporters from plants. TEVC studies of other peptide transporters showed a different voltage dependence. For AtPTR2, Ala-His- and Gly-Gly-induced currents increased almost linearly with more negative membrane potential (18). The I/V relationships of PEPT1 and PEPT2 are very complex and dependent on pH, substrate concentration, and membrane potential, and especially at lower substrate concentrations, currents saturated at negative membrane potentials and sometimes even re-approached zero. This is likely due to the fact that membrane potentials in animal cells (approximately −60 mV) are usually not as negative as the potentials observed in plant cells (27), and therefore, hyperpolarized membrane potentials are not physiologically relevant in mammals.

Substrate binding by AtPTR1 and AtPTR5 was voltage-dependent. In contrast to AtPTR2, for which the apparent affinity for Ala-Asp, Ala-Gly, and Ala-His was shown to be voltage-insensitive (pH 5.5 (18)), the dependence of the apparent affinity on membrane potential was more complex for AtPTR1 and AtPTR5. The interpretation of the effect of charge of the substrate and membrane potential on $K_{0.5}$ is not straightforward, as different steps of the transport cycle and not only the intrinsic affinity may be affected. Although at pH 5.5 the apparent affinity of AtPTR1 for Ala-Ala and Ala-Asp and of AtPTR5 for Ala-Ala and Ala-Lys remained unaffected by the membrane potential, the apparent affinity of AtPTR1 for the cationic dipeptide Ala-Lys increased, and the apparent affinity of AtPTR5 for the anionic Ala-Asp decreased with more negative membrane potentials. At pH 7.5, the apparent affinity of AtPTR1 for all three dipeptides decreased at depolarized membrane potentials. This indicates that, similar to other transporters, conformational changes in AtPTR1 and AtPTR5 are induced by membrane potential and are evident in changes in apparent substrate affinity. Therefore, membrane potential can be considered as regulating these transporters by altering substrate affinity.

The dependence of the apparent affinity of AtPTR1 on pH was similar for Ala-Ala, Ala-Lys, and Ala-Asp. Apparent affinity was highest at high $[H^+]_{out}$ and lowest at low $[H^+]_{out}$. This is different from mammalian PEPT1 and PEPT2, where the apparent affinity for positively charged peptides decreased at high $[H^+]_{out}$, and only the apparent affinity of negatively charged compounds increased at higher $[H^+]_{out}$ (16). Data on pH dependence of AtPTR2 are only available for Ala-His, again showing higher apparent affinity at low pH, as shown for the mammalian transporters (18).

The dependence of I_{max} of AtPTR1 on the external proton concentration was similar for Ala-Ala and Ala-Lys. $-I_{max}^{Ala\text{-}Ala}$ and $-I_{max}^{Ala\text{-}Lys}$ were lowest at high $[H^+]_{out}$ and increased with higher pH. Currents induced by 10 mM Ala-Ala decreased only above pH 8.5. This either reflects biophysical properties of the transporter itself at nonphysiological pH, or it represents the point at which the dependence on the co-substrate overrules these intrinsic properties of the transporter. However, it cannot be ruled out that I_{max} is not yet reached because 10 mM Ala-Ala may not be a saturating concentration at these pH values. Unfortunately, due to the nonphysiological high pH values, detailed kinetic analyses cannot be performed. A neutral pH optimum is unusual for proton-coupled transporters as proton concentration drives transport, al-

though other examples for strong regulation by pH have been described, *e.g.* AtSUC9, which is proton-coupled and has a neutral pH optimum (31). Despite these unusual properties, AtPTR1 and AtPTR5 seem to be proton-driven transporters as both a protonophore as well as a histidine-modifying agent had severe impact on peptide uptake mediated by both transporters. The effect of diethyl pyrocarbonate on the transport rate is consistent with the movement of proton(s) by protonation/deprotonation of a histidine residue as has been shown to be the case in mammalian PEPTs (23, 24). Although these histidine residues are not conserved in AtPTR1 and AtPTR5, histidine residues in other positions might have a similar function in the plant PTRs.

More [^{3}H]Ala-Ala was imported at high pH, and the presence of NaCl did not increase substrate-induced currents, indicating that higher currents are indeed due to higher peptide transport and not simply due to increased flux of cations. Thus, peptide transport is highly pH-dependent, and the lower apparent affinity of AtPTR1 for Ala-Ala and Ala-Lys at low $[H^+]_{out}$ is accompanied by a higher $-I_{max}$. In contrast, $-I_{max}^{Ala\text{-}Asp}$ of AtPTR1 was not changed from pH 5.5 to pH 7.5 and dropped only at pH 8. PEPT1 and PEPT2 also showed decreased transport at low proton concentrations (27, 32), although at saturating substrate concentrations the mammalian transporters seem to be independent of pH (16). Ala-Asp might be transported in its neutral form by AtPTR1, and therefore lack of uncharged Ala-Asp at low $[H^+]_{out}$ may result in low $-I_{max}^{Ala\text{-}Asp}$. However, more detailed studies are necessary to determine whether only uncharged Ala-Asp is transported by AtPTR1 or whether, similar to the animal transporters, both neutral and (with lower affinity) also the charged form of Ala-Asp are transported (28).

When comparing the permeability ($-I_{max}/K_m$) of AtPTR1 for dipeptides (supplemental Fig. 3), data showed that permeability increased at high $[H^+]_{out}$. At V_m −140 mV, the permeability for Ala-Lys was approximately twice as high as for Ala-Ala at all pH values, which can be explained by the fact that Ala-Lys carries a positive charge, and thus permeability of these two dipeptides *in planta* might be comparable. In contrast, at all pH values examined, the permeability for Ala-Asp was ~10-fold lower.

Taken together our data show that AtPTR1 and AtPTR5 are proton-coupled, voltage-dependent, and pH-regulated transporters that show differences in transport of dipeptides with aromatic side chains. The results also show that permeability is highest at pH and membrane potentials generally found in plant cells, indicating optimal transport under physiological conditions present *in planta*.

Acknowledgments—We are grateful to Erwin Sigel and Matthias Hediger (University of Bern) for providing Xenopus oocytes. We thank Marianne Suter Grotemeyer (University of Bern) for help with transport assays and Anke Reinders (University of Minnesota) for assistance in cRNA synthesis.

REFERENCES

1. Daniel, H., Spanier, B., Kottra, G., and Weitz, D. (2006) *Physiology* **21,** 93–102
2. Rentsch, D., Schmidt, S., and Tegeder, M. (2007) *FEBS Lett.* **581,** 2281–2289
3. Tsay, Y. F., Chiu, C. C., Tsai, C. B., Ho, C. H., and Hsu, P. K. (2007) *FEBS Lett.* **581,** 2290–2300
4. Waterworth, W. M., and Bray, C. M. (2006) *Ann. Bot.* **98,** 1–8
5. Detmers, F. J., Lanfermeijer, F. C., and Poolman, B. (2001) *Res. Microbiol.* **152,** 245–258
6. Saier, M. H., Jr. (2000) *Microbiol. Mol. Biol. Rev.* **64,** 354–411
7. Komarova, N. Y., Thor, K., Gubler, A., Meier, S., Dietrich, D., Weichert, A., Suter Grotemeyer, M., Tegeder, M., and Rentsch, D. (2008) *Plant. Physiol.* **148,** 856–869
8. Miranda, M., Borisjuk, L., Tewes, A., Dietrich, D., Rentsch, D., Weber, H., and Wobus, U. (2003) *Plant Physiol.* **132,** 1950–1960
9. West, C. E., Waterworth, W. M., Stephens, S. M., Smith, C. P., and Bray, C. M. (1998) *Plant J.* **15,** 221–229
10. Paungfoo-Lonhienne, C., Schenk, P. M., Lonhienne, T. G., Brackin, R., Meier, S., Rentsch, D., and Schmidt, S. (2009) *J. Exp. Bot.* **60,** 2665–2676
11. Segonzac, C., Boyer, J. C., Ipotesi, E., Szponarski, W., Tillard, P., Touraine, B., Sommerer, N., Rossignol, M., and Gibrat, R. (2007) *Plant Cell* **19,** 3760–3777
12. Zhou, J. J., Theodoulou, F. L., Muldin, I., Ingemarsson, B., and Miller, A. J. (1998) *J. Biol. Chem.* **273,** 12017–12023
13. Jeong, J., Suh, S., Guan, C., Tsay, Y. F., Moran, N., Oh, C. J., An, C. S., Demchenko, K. N., Pawlowski, K., and Lee, Y. (2004) *Plant Physiol.* **134,** 969–978
14. Sugiura, M., Georgescu, M. N., and Takahashi, M. (2007) *Plant Cell Physiol.* **48,** 1022–1035
15. Biegel, A., Knütter, I., Hartrodt, B., Gebauer, S., Theis, S., Luckner, P., Kottra, G., Rastetter, M., Zebisch, K., Thondorf, I., Daniel, H., Neubert, K., and Brandsch, M. (2006) *Amino Acids* **31,** 137–156
16. Daniel, H., and Kottra, G. (2004) *Pflugers Arch.* **447,** 610–618
17. Daniel, H. (2004) *Annu. Rev. Physiol.* **66,** 361–384
18. Chiang, C. S., Stacey, G., and Tsay, Y. F. (2004) *J. Biol. Chem.* **279,** 30150–30157
19. Dietrich, D., Hammes, U., Thor, K., Suter-Grotemeyer, M., Flückiger, R., Slusarenko, A. J., Ward, J. M., and Rentsch, D. (2004) *Plant J.* **40,** 488–499
20. Rentsch, D., Laloi, M., Rouhara, I., Schmelzer, E., Delrot, S., and Frommer, W. B. (1995) *FEBS Lett.* **370,** 264–268
21. Song, W., Koh, S., Czako, M., Marton, L., Drenkard, E., Becker, J. M., and Stacey, G. (1997) *Plant Physiol.* **114,** 927–935
22. Baukrowitz, T., Tucker, S. J., Schulte, U., Benndorf, K., Ruppersberg, J. P., and Fakler, B. (1999) *EMBO J.* **18,** 847–853
23. Chen, X. Z., Steel, A., and Hediger, M. A. (2000) *Biochem. Biophys. Res. Commun.* **272,** 726–730
24. Fei, Y. J., Liu, W., Prasad, P. D., Kekuda, R., Oblak, T. G., Ganapathy, V., and Leibach, F. H. (1997) *Biochemistry* **36,** 452–460
25. Fang, G., Konings, W. N., and Poolman, B. (2000) *J. Bacteriol.* **182,** 2530–2535
26. Daniel, H., Morse, E. L., and Adibi, S. A. (1992) *J. Biol. Chem.* **267,** 9565–9573
27. Chen, X. Z., Zhu, T., Smith, D. E., and Hediger, M. A. (1999) *J. Biol. Chem.* **274,** 2773–2779
28. Kottra, G., Stamfort, A., and Daniel, H. (2002) *J. Biol. Chem.* **277,** 32683–32691
29. Meharg, A. A., and Blatt, M. R. (1995) *J. Membr. Biol.* **145,** 49–66
30. Ward, J. M. (1997) *Plant Physiol.* **114,** 1151–1159
31. Sivitz, A. B., Reinders, A., Johnson, M. E., Krentz, A. D., Grof, C. P., Perroux, J. M., and Ward, J. M. (2007) *Plant Physiol.* **143,** 188–198
32. Mackenzie, B., Loo, D. D., Fei, Y., Liu, W. J., Ganapathy, V., Leibach, F. H., and Wright, E. M. (1996) *J. Biol. Chem.* **271,** 5430–5437